

**RUTHENIUM (II) COMPLEXES: PHYSICO-CHEMICAL, SPECTROSCOPIC,
REDOX, MICROBIAL AND DNA BINDING STUDIES**N. Padma Priya^a, S. Arunachalam^a, V. Chinnusamy^b and C. Jayabalakrishnan^{b*}^aDepartment of Chemistry, Kongunadu Arts and Science college, Coimbatore-641029, India.^bPost Graduate and Research Department of Chemistry, Sri Ramakrishna Mission Vidyalaya College of Arts and Science, Coimbatore-641020, India.

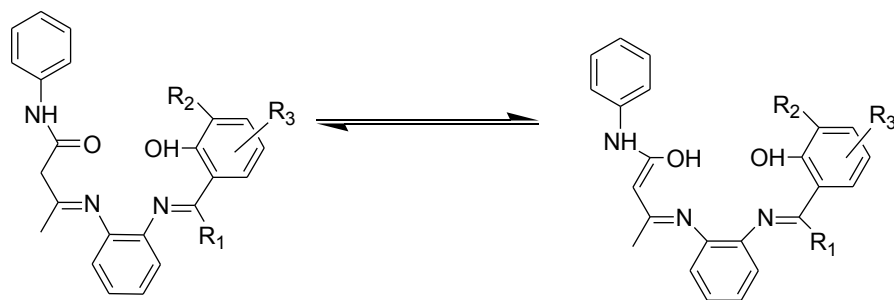
ABSTRACT : An octahedral ruthenium(II) Schiff base complexes of the type $[\text{Ru}(\text{CO})(\text{Py})\text{L}]$ (L = dianion of the Schiff bases derived from acetoacetanilide with *o*-phenylenediamine and salicylaldehyde/*o*-hydroxyacetophenone/*o*-vanillin/2-hydroxy-1-naphthaldehyde) have been synthesized from the reactions of equimolar ratio of $[\text{Ru}(\text{CO})(\text{PPh}_3)_2(\text{Py})]$ and Schiff bases in benzene. The formation of the Schiff base ligands and its complexes have been envisaged from IR, UV-VIS, ^1H , ^{13}C , ^{31}P NMR, High resolution mass and Powder XRD studies. These spectral studies confirm an octahedral environment around the metal ion. The redox behaviour of the complexes has also been determined. The ligands, metal precursors and the complexes were tested for their efficiency towards antimicrobial activity. DNA binding studies (*Herring Sperm* DNA) were carried out for the complexes $[\text{Ru}(\text{CO})(\text{Py})\text{L}^1]$ and $[\text{Ru}(\text{CO})(\text{Py})\text{L}^2]$ using biochemical techniques such as UV-VIS, cyclic voltammetry and differential pulse voltammetry. These techniques paved the way to probe the details of their DNA binding abilities. Intrinsic binding constant have been estimated and it showed a moderate intercalative interactions than the other classical intercalators.

Keywords: Ruthenium (II); redox; antimicrobial; DNA binding; intrinsic binding constant

INTRODUCTION

The design and use of the redox and spectroscopically active metal complexes as probes of DNA structure and conformation is an active area of research at the interface of chemistry and biology and these attempts have been quite fruitful [1-5]. Studies of small molecules, which react at specific sites along a DNA strand as reactive models for protein-nucleic acid interactions, provides routes toward rational drug design as well as means to develop sensitive chemical probes for DNA. A number of metal chelates have been used as probes of DNA structure in solution, as agents for mediation of strand scission of duplex DNA and as chemotherapeutic agents [6-10]. Over the past decade there has been substantial interest in the design and study of DNA binding properties of potential redox and spectroscopically active Ru(II/III) complexes [11-13] as new chemical nucleases [14-16]. The interest in determining the mode and extent of binding of metal complexes to DNA are important for understanding the cleavage properties of metal complexes in order to develop cleaving agents for probing nucleic acid structures and for other applications. Metal complexes are known to bind to DNA via both covalent and non-covalent interactions. In covalent binding the labile ligand of the complexes is replaced by a nitrogen base of DNA such as guanine N7. In fact, cisplatin, an important antitumour drug is thought to bind DNA through an intrastrand cross link between neighbouring guanine residues created by covalent binding to two soft purine nitrogen atoms. On the other hand, the non-covalent DNA interactions include intercalative, electrostatic and groove (surface) binding of cationic metal complexes along outside of DNA helix, along major or minor groove. Intercalation involves the partial insertion of aromatic heterocyclic rings of ligands between the DNA base pairs [17,18].

A number of aldehydes and ketones have been found to react with *o*-phenylenediamine leading to the formation of an azomethine linkage exhibiting a broad spectrum of biological activities [19]. Hence, in this present work we have synthesized new ruthenium(II) complexes containing *o*-phenylenediamine Schiff bases efficient for the antimicrobial and DNA binding studies. The tetradentate Schiff base ligands [20] were derived by the reaction of acetoacetanilide with *o*-phenylenediamine and salicylaldehyde/ *o*-hydroxyacetophenone/ *o*-vanillin/ 2-hydroxy-1-naphthaldehyde (Scheme 1).



R ₁	R ₂	Abbreviation
H	H	H ₂ L ¹
CH ₃	H	H ₂ L ²
H	OCH ₃	H ₂ L ³
H	H	C ₄ H ₄

Scheme 1. keto-enol form of Schiff base ligands (H₂L¹ – H₂L⁴)

EXPERIMENTAL PROCEDURE

MATERIALS

All the reagents used were of analar grade. RuCl₃.3H₂O and triphenylphosphine purchased from Loba Chemie, was used without further purification. Triphenylarsine was purchased from Sigma-Aldrich. The metal starting precursor [RuHCl(CO)(Py)(PPh₃)₂] [21] were prepared according to literature methods.

PHYSICAL MEASUREMENTS

Melting Points

Melting points were recorded on a Veego VMP-DS melting point apparatus and are uncorrected.

Elemental analyses

The analysis of carbon, hydrogen and nitrogen were performed in Vario EL III CHNS analyzer at Cochin University, Kerala, India.

IR spectra

IR spectra were recorded as KBr pellets in the 400 - 4000 cm⁻¹ region using a Perkin Elmer FT-IR 8000 spectro-photometer with a resolution of 4 cm⁻¹ in transmittance mode.

UV- VIS spectra

Electronic spectra of all the ligands and their complexes were taken in dichloromethane solution in quartz cells. The concentration of the complexes ranges around 0.02 – 0.3N. The spectra were recorded on a Systronics double beam UV-VIS Spectrophotometer 2202 in the range 200-800 nm at room temperature.

NMR spectra

^1H and ^{13}C -NMR spectra for the ligands and the complexes were recorded using Bruker 500 MHz instrument in CDCl_3 at room temperature in Indian Institute of Science, Bangalore. Minimum quantities of ligands were dissolved in deuterated CDCl_3 . ^1H -NMR chemical shifts were referenced to tetramethylsilane (TMS) as an internal solvent standard resonance and ^{13}C -NMR chemical shifts were referenced to the internal solvent resonance. ^{31}P -NMR spectra of the complexes were obtained at room temperature using o-phosphoric acid as a reference. Signals are quoted in parts per million as δ downfield from internal reference.

Mass spectra

The mass spectra were recorded using Finnigan Trace DSQ Single Quadrupole MS at SITRA, Coimbatore.

Cyclic voltammetry

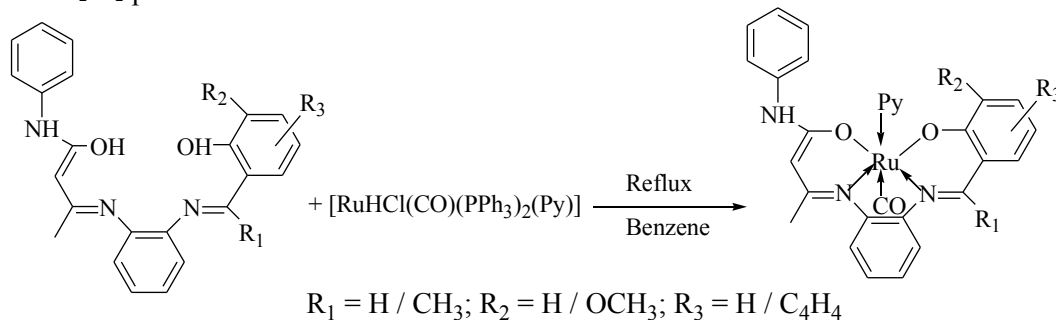
Cyclic voltammetric studies of the complexes were carried out in dichloromethane using a glassy-carbon working electrode and potentials were referenced to standard calomel electrode at Bharathiar University, Coimbatore. Minimum quantity of the complexes was dissolved in acetonitrile and decimolar solution of TBAP was added.

DNA binding studies

Concentrated stock solutions of DNA (10.5 mM) were prepared in buffer and sonicated for 25 cycles, where each cycle consisted of 30 S with 1 min intervals. The concentration of DNA in nucleotide phosphate (NP) was determined by UV absorbance at 260 nm after 1: 100 dilutions. The extinction coefficient ϵ_{260} was taken as $6600 \text{ M}^{-1} \text{ cm}^{-1}$. Stock solutions were stored at 4°C and were used within 4 days.

Synthesis of ruthenium (II) Schiff base complexes

All the new ruthenium(II) complexes were prepared by the following general procedure given below (Scheme 2). To a solution of $[\text{RuHCl}(\text{CO})(\text{Py})(\text{PPh}_3)_2]$ (0.1 mmol) in benzene (20 cm^3) the appropriate Schiff base (0.1 mmol) was added in 1:1 molar ratio and heated under reflux for about 6 hrs. The solution was then concentrated to 3 cm^3 and cooled. The complex was separated by the addition of a small amount of CH_2Cl_2 /petroleum ether and dried *in vacuo*.



Scheme 2. Synthesis of new Ru(II) Schiff base complexes

Biocidal activity

The *in vitro* antimicrobial screenings of the solvent, free ligands, metal precursors and the new ruthenium(II) complexes were tested for their effect on certain human pathogenic bacteria and fungus by disc diffusion method. The ligands, metal precursors and their ruthenium(II) complexes were stored at room temperature and dissolved in dichloromethane.

The Gram –ve (*E. coli*) bacteria were grown in Mueller Hinton agar medium and incubated at 37 °C for 48 hrs followed by frequent subculture to fresh medium and were used as test bacteria. *C. albicans* was grown in Sabourard Dextrose Agar medium were incubated at 27 °C for 72 hrs followed by periodic sub culturing to fresh medium and was used as test fungus. Then the petriplates were inoculated with a loop full of bacterial and fungal culture and spread throughout the petriplates uniformly with a sterile glass spreader. To each disc the test samples and reference antibiotic (ciprofloxacin/co-trimazine) were added with a sterile micropipette. The plates were then incubated at 35 ± 2 °C for 24 hrs for bacteria and at 27 ± 1 °C for 48 hrs for fungus, respectively. Plates with disc containing respective solvents served as control. Inhibition was recorded by measuring the diameter of the inhibitory zone after the period of incubation [22].

DNA BINDING STUDIES

Absorption titration experiments

These experiments were performed by maintaining a constant concentration of the complex while varying the nucleic acid concentration. This was achieved dissolving an appropriate amount of the metal complex in DNA stock solution and by mixing various proportions of the metal complex and DNA stock solutions while maintaining the total volume constant (1mL). This resulted in a series of solutions with varying concentrations of DNA but with a constant concentration of the complex. The absorbance (A) of the red-shifted band of the complex was recorded after successive additions of HS-DNA. The intrinsic binding constant K_b , was determined from the plot of $[DNA]/(\epsilon_a - \epsilon_f)$ Vs $[DNA]$, where $[DNA]$ is the concentration of DNA in base pairs, ϵ_a , the apparent extinction coefficient is obtained by calculating $A_{obsd}/[complex]$ and ϵ_f corresponds to the extinction coefficient of the complex in its free form. The data were fitted to (1) where ϵ_b refers to the extinction coefficient of the complex in the fully bound form.

$$[DNA]/(\epsilon_a - \epsilon_f) = [DNA]/(\epsilon_b - \epsilon_f) + 1/K_b(\epsilon_b - \epsilon_f) \text{ -----(1)}$$

Each set of data, when fitted to the above equation, gave a straight line with a slope of $1/(\epsilon_b - \epsilon_f)$ and a y-intercept of $1/K_b(\epsilon_b - \epsilon_f)$. K_b was determined from the ratio of the slope to intercept. Microcal Origin software package was used for curve fitting the data [23].

Electrochemical titration experiments

Cyclic voltammetry (CV) and differential pulse voltammetry (DPV) were performed using a three electrode cell configuration. The studies were carried out in acetonitrile using a glassy-carbon working electrode and potentials were referenced to standard calomel electrode respectively. The supporting electrolyte used was NBu_4ClO_4 . The E_{pa} values were observed under identical conditions [24].

RESULTS AND DISCUSSION

The tetradentate Schiff bases (H_2L^1 - H_2L^4) react with the metal precursors of the general formula $[RuHCl(CO)(PPh_3)_2(Py)]$ in 1: 1 molar ratio in benzene to yield the complexes of the type $[Ru(CO)(Py)L]$ (Scheme 2). The new complexes were soluble in most of the common organic solvents and their purity was checked by TLC. From the TLC, we obtained a single spot which confirmed that there were no isomers in the metal complexes. This fact is further supported by the analytical data obtained for all the new complexes which agreed well with proposed molecular formulae (Table 1). We have attempted to prepare single crystals of the metal complexes in different solvents, but we could not prepare convenient single crystals of the complexes.

Table.1. Analytical data of Ru (II) Schiff base complexes

Ligands and Complexes	Colour	Melting point (°C)	Empirical formula	Molecular weight	Elemental analysis Calculated (found) (%)		
					C	H	N
H ₂ L ¹	Orange	62	C ₂₃ H ₂₁ N ₃ O ₂	371.422	74.38(74.35)	5.70(5.69)	11.31(11.28)
H ₂ L ²	Brown	71	C ₂₄ H ₂₃ N ₃ O ₂	385.449	74.79(74.73)	6.01(6.03)	10.90(10.87)
H ₂ L ³	Brown	69	C ₂₄ H ₂₃ N ₃ O ₃	401.439	71.81(71.80)	5.76(5.77)	10.47(10.45)
H ₂ L ⁴	Orange	64	C ₂₇ H ₂₃ N ₃ O ₂	421.482	76.94(76.90)	5.50(5.49)	9.97(9.95)
[Ru(CO)(Py)L ¹]	Green	188	RuC ₂₉ H ₂₄ N ₄ O ₃	577.579	60.31(60.30)	4.19(4.17)	9.70(9.69)
[Ru(CO)(Py)L ²]	Green	118	RuC ₃₀ H ₂₆ N ₄ O ₃	591.606	60.91(60.89)	4.43(4.42)	9.47(9.48)
[Ru(CO)(Py)L ³]	Green	170	RuC ₃₀ H ₂₆ N ₄ O ₄	607.596	59.30(59.27)	4.31(4.32)	9.22(9.20)
[Ru(CO)(Py)L ⁴]	Brown	120	RuC ₃₃ H ₂₆ N ₄ O ₃	627.639	63.15(63.14)	4.18(4.19)	8.93(8.90)

FT-IR spectral analysis

The preliminary identification regarding the formation of the free Schiff base ligands and its complexes were obtained from IR spectral data (Table 2). A strong band observed around 1710 cm⁻¹ in the free Schiff base ligands due to $\nu_{C=O}$ completely disappeared on complexation. This may be due to the enolisation and subsequent coordination through the deprotonated enolised oxygen atom [25,26]. The free Schiff base ligand shows a very strong absorption at 1619-1664 cm⁻¹ which is characteristic of the azomethine $\nu_{C=N}$ group. In the Schiff base complexes, the absorption has been shifted to the region 1599-1606 cm⁻¹ indicating the coordination of the Schiff bases through the nitrogen atom of the phenolic moiety [27]. In all the complexes, the bands in the region 1434-1468 cm⁻¹ have been assigned to the mixed vibrational mode arising from $\nu_{C=N}$ and $\nu_{C=CH}$. This is indicative of coordination of the Schiff base nitrogen atom to the metal ion [28]. Another medium intensity band around 3000 cm⁻¹ in the free ligands due to phenolic ν_{OH} was absent in the complexes indicating the deprotonation of the Schiff bases prior to the coordination. This fact is further supported by the increase in the absorption frequency of the phenolic ν_{C-O} from 1243-1261 cm⁻¹ in the free ligands to 1262-1325 cm⁻¹ in the ruthenium complexes confirming the other coordination site of Schiff base is the phenolic oxygen atom [29,30]. In all the complexes, a strong band appears in the region 1936-1954 cm⁻¹ owing to the terminal carbonyl group [31]. All the complexes showed a medium intensity band in the 1021-1030 cm⁻¹ region characteristic of the coordinated pyridine. The coordination of the azomethine nitrogen and phenolic oxygen atoms are further supported by the appearance of two bands at 414-456 cm⁻¹ and 516-535 cm⁻¹ due to ν_{M-N} and ν_{M-O} respectively [32,33]. From the IR spectral data, we inferred that the Schiff bases behave as dibasic tetradentate ligands.

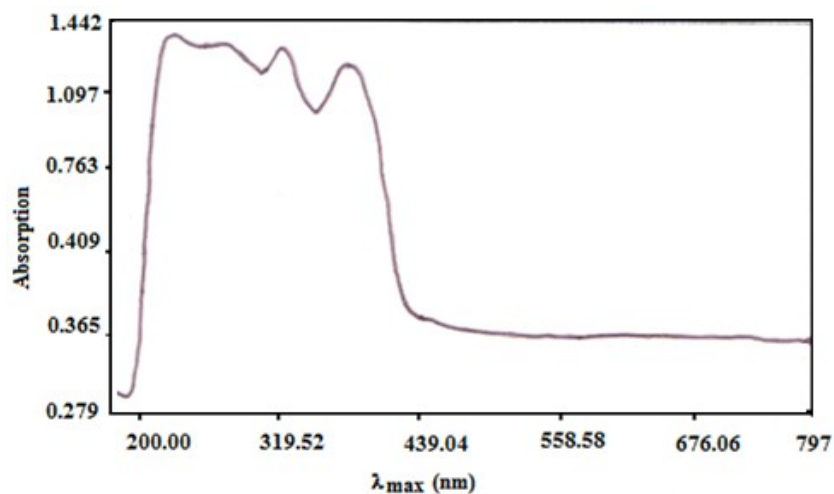
Electronic spectral analysis

The electronic spectral data of the free ligands and their complexes in CH₂Cl₂ were recorded and the values are listed in Table 2 and Figure 1. The spectra of the ligand showed two types of transitions namely $\pi-\pi^*$ and $n-\pi^*$ in the range 298-304 nm and 349-480 nm respectively for the electrons localized on the benzene ring, C=N, phenolic OH and enolic OH of the Schiff bases. The spectra of the complexes showed three to six bands in the region 254-474 nm. All the Schiff base ruthenium complexes were diamagnetic, indicating the presence of ruthenium in the +2 oxidation state. The ground state of ruthenium(II) in an octahedral environment is ¹A_{1g}, arising from the t_{2g}⁶ configuration and the excited states corresponding to the t_{2g}⁵ e_g¹ configuration were ³T_{1g}, ³T_{2g}, ¹T_{1g} and ¹T_{2g}. Hence, four bands corresponding to the transitions ¹A_{1g}→³T_{1g}, ¹A_{1g}→³T_{2g}, ¹A_{1g}→¹T_{1g} and ¹A_{1g}→¹T_{2g} are possible in the order of increasing energy. The other high intensity band in the visible region 254-484 nm was assigned as charge transfer transitions arising from the metal t_{2g} level to the unfilled π^* molecular orbital of the ligand. This pattern of the electronic spectra of all the complexes indicate the presence of an octahedral environment around the ruthenium(II) ion which is similar to other ruthenium(II) octahedral complexes [33-37].

Table.2. FT-IR, UV-vis and Electrochemical data of new Ru(II) Schiff base complexes

Ligands and Complexes	IR spectra(cm^{-1})				$\lambda_{\text{max}}(\text{nm})$	*Electrochemical data ($\text{Ru}^{\text{II}} - \text{Ru}^{\text{I}}$)				($\text{Ru}^{\text{II}} - \text{Ru}^{\text{III}}$)
	$\nu_{\text{C}=\text{N}}$	$\nu_{\text{Ph-C-O}}$	$\nu_{\text{C}=\text{CH}+\nu_{\text{C}=\text{N}}}$	$\nu_{\text{C}=\text{O}}$		$E_{\text{pa}}(\text{V})$	$E_{\text{pc}}(\text{V})$	$E_{\text{r}}(\text{V})$	$\Delta E_{\text{p}}(\text{mV})$	$E_{\text{pc}}(\text{V})$
H_2L^1	1664	1261	-	-	299,368,395	-	-	-	-	-
H_2L^2	1641	1243	-	-	298,304,362,395,458	-	-	-	-	-
H_2L^3	1619	1255	-	-	299,349	-	-	-	-	-
H_2L^4	1620	1245	-	-	304,368,414,445,480	-	-	-	-	-
$[\text{Ru}(\text{CO})(\text{Py})\text{L}^1]$	1599	1321	1442	1940	258,301,398	-1.62	-0.23	-0.925	1300	0.90
$[\text{Ru}(\text{CO})(\text{Py})\text{L}^2]$	1599	1262	1434	1954	258,283,391	-1.592	-1.56	-1.576	32	0.80
$[\text{Ru}(\text{CO})(\text{Py})\text{L}^3]$	1599	1263	1515	1942	258,297,348,402	-0.349	-0.239	-0.294	110	0.93
$[\text{Ru}(\text{CO})(\text{Py})\text{L}^4]$	1606	1325	1468	1941	254,297,369,405,438,474	-1.635	-1.612	-1.624	23	0.94

*Supporting electrolyte: $[\text{NBu}_4]\text{ClO}_4$ (0.1M); Scan rate, 0.1 mV^{-1} ; reference electrode, Ag-AgCl. $\Delta E_{\text{p}} = E_{\text{pa}} - E_{\text{pc}}$; $E_{1/2} = 0.5 (E_{\text{pa}} + E_{\text{pc}})$, Where E_{pa} and E_{pc} are the anodic and cathodic peak potentials in Volts, respectively.

Figure 1. Electronic spectrum of the complex $[\text{Ru}(\text{CO})(\text{Py})\text{L}^3]$

^1H , ^{13}C and ^{31}P NMR spectral analysis

The ^1H NMR spectra of the free Schiff base ligands and the complexes (Table 3) were recorded in CDCl_3 solution. In the Schiff base ligands (Figure 2), the aromatic protons appear as multiplet in the range 7.0-8.0 ppm. The NH, enolic OH, methine and methyl protons of the acetanilide moiety appears as singlet in the range 3.5, 15.0-15.3, 2.2-2.3 and 0.9-1.2 ppm respectively. The azomethine proton of the ligands H_2L^1 , H_2L^3 and H_2L^4 appear as a singlet at 8.6 ppm. The $-\text{N}=\text{C}-\text{CH}_3$ protons of H_2L^2 ligand appear as singlet at 0.9 ppm. In H_2L^3 ligand, the methoxy protons appear as singlet at 2.0 ppm. The phenolic OH proton appears as singlet in the range 9.8-10.3 ppm.

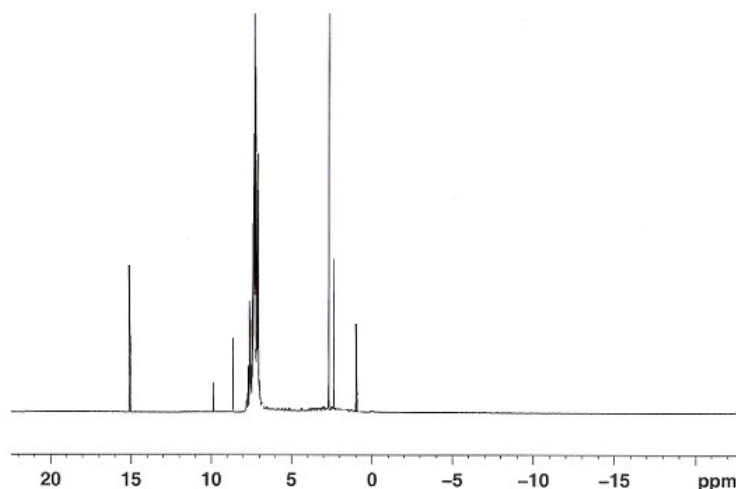


Figure 2. ^1H NMR spectrum of the Schiff base Ligand H_2L^1

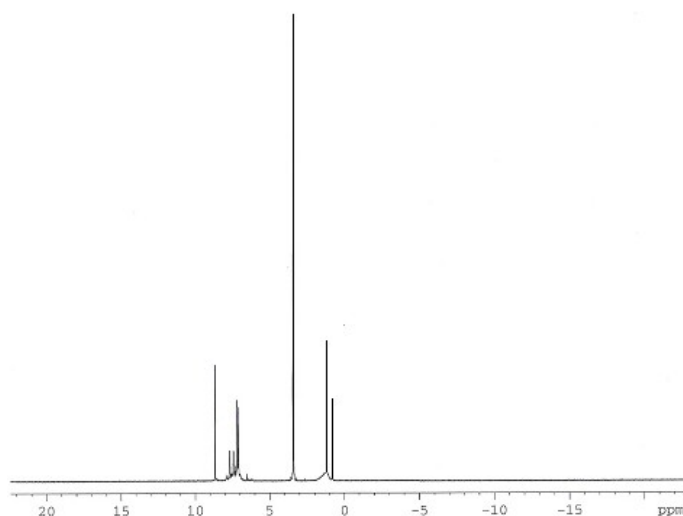
For the ruthenium(II) complexes (Figure 3), multiplets observed in the range 6.2-8.2 ppm have been assigned for the aromatic protons of phenyl, naphthalene, triphenylphosphine, triphenylarsine and pyridine moieties [38]. In all the complexes, the NH, methine and methyl protons of the acetanilide moiety appear as a singlet in the region 3.0-3.5, 1.2-2.2 and 0.8-1.6 ppm respectively. For the complexes of the corresponding H_2L^1 , H_2L^3 and H_2L^4 ligands, the azomethine proton appear as singlet at 8.6-8.7 ppm. The azomethine methyl carbon of the phenolic moiety for the complex $[\text{Ru}(\text{CO})(\text{Py})\text{L}^2]$ appear as singlet at 1.2 ppm. For the complexes $[\text{Ru}(\text{CO})(\text{PPh}_3)\text{L}^3]$ and $[\text{Ru}(\text{CO})(\text{Py})\text{L}^3]$, the methoxy carbon appear as a singlet at 1.9 ppm.

The ^{13}C NMR spectra of the ligands and the complexes (Table 3) were recorded in CDCl_3 solution and revealed the presence of expected number of signals corresponding to different types of carbon atoms present in the complexes. In the free ligands, the aromatic carbons appear in the range 119-138 ppm. The enolic, methine and methyl carbons of the acetanilide moiety appear at 65.8-72.4, 32.2-56.3 and 14.9-20.4 ppm respectively. The azomethine carbon of the acetanilide moiety appears at 150.08-159.2 ppm. For all the ligands, the azomethine carbon of the phenolic moiety appears at 163.6-168.6 ppm. The methyl and methoxy carbons of the phenolic moiety for the ligands H_2L^2 and H_2L^3 appears at 24.5 ppm and 29.8 ppm respectively.

For the complexes (Figure 4), the aromatic carbons appear at 120-138 ppm. The enolic, methine and methyl carbons of the acetanilide moiety appear at 71.8-73.8, 45.5-55.6 and 18.2-19.5 ppm respectively. The azomethine carbon of the acetanilide moiety appears at 150.1-155.7 ppm. The azomethine carbon of the phenolic moiety appears in the range 160.6-163.0 ppm. The methyl and methoxy carbon for the corresponding complexes of the ligands L^2 and L^3 appear at 24.5 and 20.2 ppm. For all the complexes, the free $\text{C}\equiv\text{O}$ carbon appears in the range 171.3-176.3 ppm.

Table 3. ^1H and ^{13}C – NMR spectral data of Ru(II) Schiff base complexes

Ligands and Complexes	^1H -NMR (ppm)	^{13}C -NMR (ppm)
H_2L^1	7.0-7.7(m, ar), 3.5(s, NH), 15.0(s, enolic-OH), 2.3(s, CH), 1.2(s, CH_3), 8.6(s, $\text{HC}=\text{N}$), 9.9(s, Ph-OH)	119-138 (aromatic C), 70.0 (enolic C-OH), 32.2 (CH), 20.4 (CH_3), 159.2 (anilide C=N), 163.6 (phenolic $\text{HC}=\text{N}$)
H_2L^2	7.0-7.5(m, ar), 3.5(s, NH), 15.1(s, enolic-OH), 2.2(s, CH), 1.1(s, CH_3), 0.9(s, $\text{CH}_3\text{-C}=\text{N}$), 10.1(s, Ph-OH)	120-138 (aromatic C), 70.2 (enolic C-OH), 54.8 (CH), 14.9 (CH_3), 151.09 (anilide C=N), 168.59(phenolic C=N), 24.5 (CH_3)
H_2L^3	7.0-7.8(m, ar), 3.5(s, NH), 15.3(s, enolic-OH), 2.2(s, CH), 1.2(s, CH_3), 8.6(s, $\text{HC}=\text{N}$), 10.3(s, Ph-OH), 2.0(s, OCH_3)	119-129 (aromatic C), 65.8 (enolic C-OH), 56.3 (CH), 15.0 (CH_3), 150.08 (anilide C=N), 165.68 (phenolic $\text{HC}=\text{N}$), 29.82 (OCH_3)
H_2L^4	7.0-8.0(m, ar), 3.5(s, NH), 15.1(s, enolic-OH), 2.2(s, CH), 0.9(s, CH_3), 8.6(s, $\text{HC}=\text{N}$), 9.8(s, Ph-OH)	119-138 (aromatic C), 72.4 (enolic C-OH), 40.0 (CH), 20.2 (CH_3), 159.2 (anilide C=N), 164.6 (phenolic $\text{HC}=\text{N}$)
$[\text{Ru}(\text{CO})(\text{Py})\text{L}^1]$	6.8-7.9(m, ar), 3.4(s, NH), 1.2(s, CH), 0.8(s, CH_3), 8.6(s, $\text{HC}=\text{N}$),	127-134 (aromatic C), 72.0 (enolic C-O), 50.4 (CH), 20.0 (CH_3), 155.7 (anilide C=N), 163.0 (phenolic $\text{HC}=\text{N}$), 172.0 (C=O)
$[\text{Ru}(\text{CO})(\text{Py})\text{L}^2]$	6.2-8.0(m, ar), 3.0(s, NH), 2.2(s, CH), 1.6(s, CH_3), 1.2(s, $\text{N}=\text{C}-\text{CH}_3$)	120-131 (aromatic C), 73.8 (enolic C-O), 55.3 (CH), 18.2 (CH_3), 153.2 (anilide C=N), 161.6 (phenolic C=N), 24.5 (CH_3), 176.3 (C=O)
$[\text{Ru}(\text{CO})(\text{Py})\text{L}^3]$	6.7-7.8(m, ar), 3.5(s, NH), 2.2(s, CH), 1.5(s, CH_3), 8.7(s, $\text{HC}=\text{N}$), 1.9(s, Ph- OCH_3)	124-130 (aromatic C), 71.8 (enolic C-O), 45.5 (CH), 19.5 (CH_3), 153.6 (anilide C=N), 164.1(phenolic C=N), 20.2 (OCH_3), 176.2 (C=O)
$[\text{Ru}(\text{CO})(\text{Py})\text{L}^4]$	6.2-8.2(m, ar), 3.5(s, NH), 1.6(s, CH), 0.9(s, CH_3), 8.6(s, $\text{HC}=\text{N}$),	124-138 (aromatic C), 72.3 (enolic C-O), 55.6 (CH), 18.6 (CH_3), 150.1 (anilide C=N), 160.6 (phenolic $\text{HC}=\text{N}$), 171.3 (C=O)

Figure 3. ^1H NMR spectra of the complex $[\text{Ru}(\text{CO})(\text{Py})\text{L}^1]$

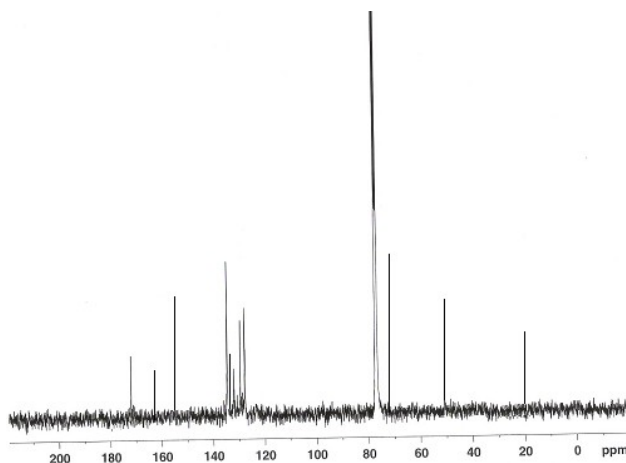


Figure 4. ^{13}C NMR spectra of the complex $[\text{Ru}(\text{CO})(\text{Py})\text{L}^1]$

The ^{31}P NMR spectra were recorded for two complexes in order to confirm the presence of PPh_3 . The complex $[\text{Ru}(\text{CO})(\text{Py})\text{L}^1]$ exhibits no peak, confirming the absence of the PPh_3 group. This indicates the retention of coordinated pyridine in the new complexes even after the coordination of tetradentate Schiff bases [38].

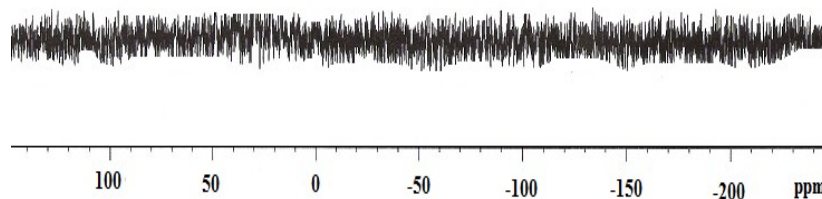


Figure 5. ^{31}P NMR spectra of the complex $[\text{Ru}(\text{CO})(\text{Py})\text{L}^1]$

Mass spectral analysis

The high resolution mass spectra of $[\text{Ru}(\text{CO})(\text{Py})\text{L}^3]$ displayed molecular ion peak at m/z 607.5961. Similarly, the molecular ion peak of the complex $[\text{Ru}(\text{CO})(\text{PPh}_3)\text{L}^4]$ appeared at m/z 810.8200. These molecular ion peaks are consistent with the proposed molecular formula of the corresponding ruthenium(II) Schiff base complexes [39].

Electrochemical studies

Electrochemical study were carried out for all the complexes in dichloromethane solution at a glassy carbon working electrode and the potentials were expressed with reference to $\text{Ag}-\text{AgCl}$ (Table 2). The reduction of each complex was characterized by well defined waves with E_r values observed in the range -0.925 to -1.624 mV (reduction). The complexes $[\text{Ru}(\text{CO})(\text{Py})\text{L}^1]$ and $[\text{Ru}(\text{CO})(\text{Py})\text{L}^3]$ showed reduction couples with peak to peak separation values (ΔE_p) ranging from 110-1300 mV revealing that this process is quasi-reversible in nature. This is attributed to slow electron transfer and adsorption of the complexes onto the electrode surface [33].

For the remaining complexes, the peak to peak separation value (ΔE_p) fell in the range 23-32 mV suggesting a reversible one-electron transfer process. The oxidation couple for the entire complex is irreversible. The reason for the irreversibility of these complexes may be due to oxidative degradation or the short-lived oxidized state of the metal ion [40].

Table 4. Antibacterial and antifungal activities of Ru(II) complexes

Ligands, Metal starting precursors and Complexes	Diameter of inhibition zone (mm)							
	Antibacterial activity (<i>E. coli</i>)				Antifungal activity (<i>C. albicans</i>)			
	0.25%	0.5%	1.0%	2.0%	0.25%	0.5%	1.0%	2.0%
[RuHCl(CO)(Py)(PPh ₃) ₂]	7	8	9	9	5	7	7	7
H ₂ L ¹	2	2	3	3	-	-	-	1
H ₂ L ²	2	3	3	4	-	-	1	3
H ₂ L ³	-	3	3	3	-	-	-	2
H ₂ L ⁴	1	2	2	3	-	1	2	2
[Ru(CO)(Py)L ¹]	13	13	14	14	9	9	9	10
[Ru(CO)(Py)L ²]	18	18	20	21	15	16	18	20
[Ru(CO)(Py)L ³]	14	14	14	15	12	12	13	13
Standard*	20	20	21	21	15	17	19	20
Solvent	No activity							

*Ciprofloxacin- for bacterial / Co-trimazine- for fungi

Microbial activity

The *in vitro* antimicrobial screenings of the free ligands, metal precursors and its ruthenium (II) complexes were tested for their effect on certain human pathogenic bacteria and fungus (Table 5). The variation in the effectiveness of the different compounds against different organisms depends on their impermeability of the microbial cells or on the difference in the ribosome of the microbial cells [41]. All the complexes show better antibacterial and antifungal activity when compared to the free ligands and metal precursors. The increase in the microbial activity of the metal complexes with increase in concentration is due to the effect of metal atom on normal cell process. Such increased activity of the metal complexes can be explained on the basis of overtone's concept [42] and chelation theory [43,44]. According to overtone's concept of cell permeability, the lipid membrane that surrounds the cell favours the passage of only lipid soluble materials due to which liposolubility has an important factor which controls the antimicrobial activity. On chelation, the polarity of the metal atom will be reduced to a greater extent due to the overlap of the ligand orbital and partial sharing of positive charge of metal atom with donor groups. Further, it increases the delocalization of π electrons over the whole chelate ring and enhances the lipophilicity which enhances the penetration of the complexes. This increased lipophilicity enhances the penetration of the complexes into lipid membrane and blocking the metal binding-sites on enzymes of microorganisms.

These complexes may disturb the respiration process of the cell and thus block the synthesis of proteins which restrict the further growth of the organism [45]. The complexes $[\text{Ru}(\text{CO})(\text{Py})\text{L}^1]$ and $[\text{Ru}(\text{CO})(\text{Py})\text{L}^2]$ showed higher biological activity than other complexes. Among them the complex $[\text{Ru}(\text{CO})(\text{Py})\text{L}^2]$ showed higher activity due to the presence of electron donating methyl group in the phenyl substituent of the Schiff base ligands [46,47]. So we intend to test the DNA binding ability of these complexes.

Table 5. DNA binding studies of the complexes $[\text{Ru}(\text{CO})(\text{Py})\text{L}^1]$ and $[\text{Ru}(\text{CO})(\text{Py})\text{L}^2]$

Complexes	R (R= [DNA]/[complex])	UV-Vis (λ_{max}) nm	Cyclic Voltammetry $\text{Ru}^{\text{II}}-\text{Ru}^{\text{I}}$ E_{pa} (mV)	Differential Pulse Voltammetry (mV)
$[\text{Ru}(\text{CO})(\text{Py})\text{L}^1]$	0.0	255	-845.524	-842.016
	0.2	256	-853.297	-847.707
	0.4	257	-856.319	-857.942
	0.6	258	-859.947	-865.933
	0.8	258	-862.845	-869.383
	1.0	259	-876.181	-876.801
$[\text{Ru}(\text{CO})(\text{Py})\text{L}^2]$	0.0	254	-855.339	-863.191
	0.2	255	-860.529	-869.123
	0.4	257	-861.319	-871.622
	0.6	259	-862.947	-872.648
	0.8	260	-869.405	-876.128
	1.0	261	-876.723	-880.634

Measured vs. Ag/AgCl electrode: scan rate: 50 mV: supporting electrolyte 5mM Tris- HCl/ 50mM NaCl: complex concentration 100 μM . Based on $E_{1/2}$ values from DPV measurements, scan rate: 1mV s⁻¹, pulse height 50mV.

DNA binding studies

a) UV-vis spectroscopy

UV- vis absorption studies were performed to ascertain the DNA-complexes $[\text{Ru}(\text{CO})(\text{Py})\text{L}^1]$, $[\text{Ru}(\text{CO})(\text{Py})\text{L}^2]$ interaction (Table 6, Figure 6) . The UV-absorbance showed an increase with the increase in drug concentration. Since, the complex does not show any peak at 260 nm, the rise in the DNA absorbance is indicative of the complex formation between DNA and the complex molecules [19]. Addition of increasing amount of DNA results in an appreciable increase in the absorption intensity of MLCT band with very small red shift in wavelength. The hyperchromism in the MLCT band reaches 27.5%, due to distortions in the DNA helix, caused by firmly bound or intercalated metal complexes [49-51]. So we primarily speculate that the complex interaction with the secondary structure of the *HS*-DNA results in its breakage and perturbation. The intrinsic binding constant of the complexes $[\text{Ru}(\text{CO})(\text{Py})\text{L}^1]$ and $[\text{Ru}(\text{CO})(\text{Py})\text{L}^2]$ K_b were found to be $4.018 \times 10^3 \text{ M}^{-1}$ and $2.323 \times 10^4 \text{ M}^{-1}$ respectively. No isobestic points are observed for the complex while binding to DNA suggesting that the complexes exhibit a single mode of binding to DNA [52]. This is indicative of binding of the complexes $[\text{Ru}(\text{CO})(\text{Py})\text{L}^1]$ and $[\text{Ru}(\text{CO})(\text{Py})\text{L}^2]$ with DNA host with lower affinity than the other classical intercalators.

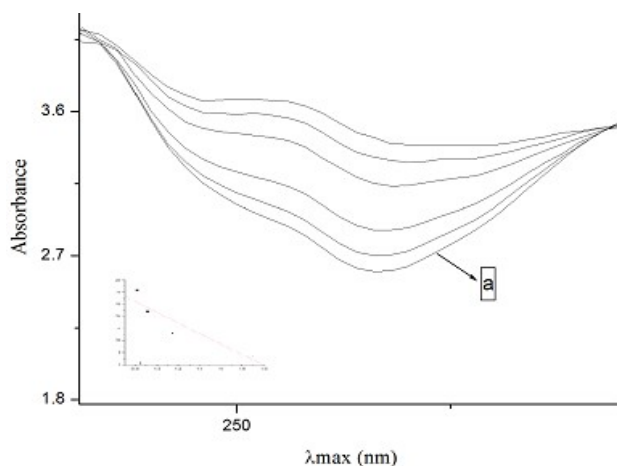


Figure 6. Absorption spectra of $[\text{Ru}(\text{CO})(\text{Py})\text{L}^2]$ complex ($100 \mu\text{M}$) in aqueous Tris buffer (5 mM Tris HCl, 50 mM NaCl, pH 7.1) upon the addition of herring sperm DNA ($0-100 \mu\text{M}$), a – absence of DNA

Electrochemical studies

Electrochemical methods are widely used to study the interaction of DNA with metal chelates. Based on the shift of potential in the cyclic voltammograms, the interaction mode of compounds with DNA can be inferred [52]. The application of cyclic voltammetry (CV) and differential pulse voltammetry (DPV) to the study of binding of metal complexes to DNA provides a useful complement to the methods of investigations such as UV-VISIBLE spectroscopy [19,52]. For the complexes $[\text{Ru}(\text{CO})(\text{Py})\text{L}^1]$ and $[\text{Ru}(\text{CO})(\text{Py})\text{L}^2]$, reduction of $\text{Ru}^{\text{II}}-\text{Ru}^{\text{I}}$ shows a irreversible reduction potential with E_{pa} values from -845.524 to -862.845 mV and -863.191 to -880.634 mV respectively (Table 7) and is depicted in Figure 7. Since $\text{Ru}^{\text{II}}-\text{Ru}^{\text{I}}$ couples exhibit irreversible values even at $R = 0$ ($R = [\text{DNA}] / [\text{Ru}(\text{CO})(\text{Py})\text{L}^2]$), no attempt was made to calculate the binding constant from CV. Upon addition of DNA, the complexes $[\text{Ru}(\text{CO})(\text{Py})\text{L}^1]$ and $[\text{Ru}(\text{CO})(\text{Py})\text{L}^2]$ experience a negative shift in E_{pa} of 31 mV and 21 mV . The observed shift in E_{pa} of 35 mV and 17 mV values (DPV) (Figure 8) to less negative potentials suggest that both $\text{Ru}(\text{II})$ and $\text{Ru}(\text{I})$ forms of the complexes bind to DNA but $\text{Ru}(\text{I})$ display a higher DNA binding affinity than $\text{Ru}(\text{II})$ form.

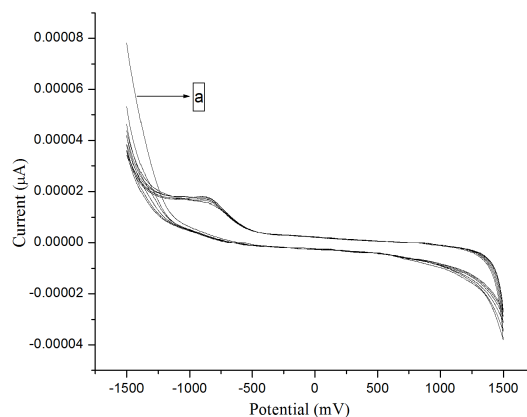


Figure 7. Cyclic voltammograms of the complex $[\text{Ru}(\text{CO})(\text{Py})\text{L}^2]$ in the absence and in presence of DNA at the scan rate of 100 mVs^{-1} , in Tris-HCl buffer pH 7.1, a – absence of DNA

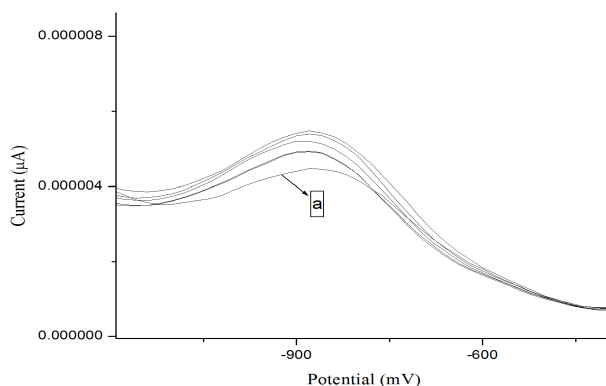
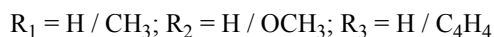
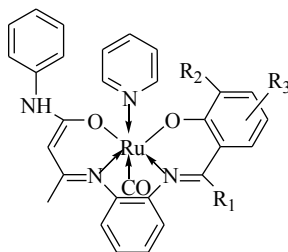


Figure 8. Differential pulse voltammograms (DPV) of the complex $[\text{Ru}(\text{CO})(\text{Py})\text{L}^2]$ with increasing concentration of DNA, a – absence of DNA

Conclusions

New diamagnetic ruthenium(II) complexes of the type $[\text{Ru}(\text{CO})(\text{B})(\text{L})]$ were synthesized and characterized by elemental analysis, spectral (FT-IR, UV-VIS, ^1H , ^{13}C , ^{31}P -NMR and Mass) and cyclic voltammetric studies. Based on the analytical and spectroscopic studies, an octahedral geometry has been tentatively proposed for all the ruthenium (II) complexes (Scheme 3).



Scheme 3. General structure of Ru(II) Schiff base complexes

The biocidal efficiency of the complexes has also been evaluated and found that the Ru(II) Schiff base complexes show better biological activity when compared with the Schiff base ligands and the metal precursors. The complexes ($[\text{Ru}(\text{CO})(\text{Py})\text{L}^1]$ $[\text{Ru}(\text{CO})(\text{Py})\text{L}^2]$) showed higher biological efficiency when compared to the remaining complexes and it also reached the effectiveness of the standards ciprofloxacin and co-trimazine. The presence of electron donating group in the phenyl ring enhanced the activity of the complex $[\text{Ru}(\text{CO})(\text{Py})\text{L}^2]$ than the complex $[\text{Ru}(\text{CO})(\text{Py})\text{L}^1]$. Usually, the electron donating substituents increases the biological activities. Hence as a further study, we investigated the binding ability of these complexes with the DNA. From the UV and electrochemical titration experiments, we inferred that the complexes $[\text{Ru}(\text{CO})\text{Py}(\text{L}^1)]$ and $[\text{Ru}(\text{CO})(\text{Py})\text{L}^2]$ was able to bind DNA (*Herring Sperm*) with higher affinity in Ru(I) oxidation state and the binding constant found by UV-VIS study K_b is $4.018 \times 10^3 \text{ M}^{-1}$ and $2.323 \times 10^4 \text{ M}^{-1}$ which was less when compared with the other classical intercalators. The $[\text{Ru}(\text{CO})(\text{Py})\text{L}^2]$ shows higher binding activity due to the presence of electron donating methyl group in the phenolic moiety [46,47].

REFERENCES

1. L. N. Ji, X. H. Zou, J. G. Lin, *Coord. Chem. Rev.* 2001, 513, 216.
2. I. Antonini, P. Polucci, A. Magnano, G. Barbara, M. Palumbo, E. Menta, N. Pescalli, S. Martelli, *J. Med. Chem.* 2002, 45, 697.
3. H. L. Chan, H. Q. Lin, B. C. Tzeng, Y. S. You, S. M. Peng, M. Yang, C. M. Che, *Inorg. Chem.* 2002, 41, 3161.
4. J. Z. Wu, H. Li, J. G. Zhang, J. H. Ku, *Inorg. Chem. Commun.* 2002, 5, 71.
5. J. N. Burstyn, J. H. Bernays, S. M. Cohen, S. J. Lippard, *Nucleic Acids Res.* 2000, 28, 4237.
6. J. A. Cowan, *Curr. Opin. Chem. Biol.* 2001, 5, 634.
7. J. K. Barton, *Science* 1986, 223, 727.
8. S. Dhar, A. R. Chakravarthy, *Inorg. Chem.* 2003, 42, 2483.
9. L. P. Lu, M. L. Zhu, P. Yang, *J. Inorg. Biochem.* 2003, 95, 31.
10. J. Z. Wu, H. Li, J. G. Zhang, J. H. Xu, *Inorg. Chem. Commun.* 2002, 5, 71.
11. J. Liu, W. J. Mei, L. J. Lin, K. C. Zheng, H. Chao, F. C. Yun, L. N. Ji, *Inorg. Chim. Acta* 2004, 357, 285.
12. H. Chao, W. J. Mei, Q. W. Huang, L. N. Ji, *J. Inorg. Biochem.* 2002, 92, 165.
13. J. Z. Wu, L. Yuan, *J. Inorg. Biochem.* 2004, 98, 41.
14. R. Nagane, M. Chilcira, H. Shindo, W. E. Antholine, *J. Inorg. Biochem.* 2000, 78, 243.
15. D. K. Chand, H. J. Schneider, J. A. Agnilar, F. Escarti, E. G. Espana, S. V. Luis, *Inorg. Chim. Acta* 2001, 316, 71.
16. P. M. Bush, J. P. Whitehead, C. C. Pink, E. C. Gramm, J. L. Eglin, P. S. Watton, E. L. Pence, *Inorg. Chem.* 2001, 40, 1871.
17. M. Chikira, Y. Tomizava, D. Fukita, T. Sugizaki, N. Sugawara, T. Yamazaki, A. Sasano, S. Shindo, M. Palaniandavar, W. E. Antholine, *J. Inorg. Biochem.* 2002, 89, 163.
18. A. Raja, V. Rajendiran, P. Uma Maheswari, R. Balamurugan, C. A. Kilner, M. A. Halcrow, M. Palaniandavar, *J. Inorg. Biochem.* 2005, 99, 1717.
19. M. Shakir, M. Azam, Y. Azim, S. Parveen, A. U. Khan, *Polyhedron* 2007, 26, 5513.
20. N. Padma Priya, S. Arunachalam, A. Manimaran, D. Muthupriya, C. Jayabalakrishnan, *Spectrochim. Acta Part A* 2009, 72, 670.
21. S. Gopinathan, I. R. Unny, S. S. Deshpande, C. Gopinathan, *Ind. J. Chem.* 1986, 25A, 1015.
22. S. Kannan, M. Sivagamasundari, R. Ramesh, Y. Liu, *J. Organomet. Chem.* 2008, 693, 2251.
23. S. Arounaguri, D. Easwaramoorthy, A. Ashokkumar, A. Dattagupta, B.G. Maiya, *J. Chem. Sci.* 2000, 112, 1.
24. B. Selvakumar, V. Rajendiran, P. Uma Maheswari, H. S. Evans, M. Palaniandavar, *J. Inorg. Biochem.* 2006, 100, 316.
25. K. P. Balasubramanian, R. Karvembu, V. Chinnusamy, K. Natarajan, *Ind. J. Chem.* 2005, 44A, 2450.
26. K. P. Balasubramanian, R. Karvembu, R. Prabhakaran, V. Chinnusamy, K. Natarajan, *Spectrochim. Acta part A* 2007, 68, 50.
27. G. Gupta, R. Sharon, R. K. Kapoor, *Trans. Met. Chem.* 1978, 3, 282.
28. R. Karvembu, K. Natarajan, *Polyhedron* 2002, 21, 1721.
29. B. Khera, A. K. Sharma, N. K. Kaushik, *Polyhedron* 1983, 2, 1177.
30. R. Prabhakaran, V. Krishnan, K. Pasumpon, D. Sukanya, E. Wendel, C. Jayabalakrishnan, H. Bertagnolli, K. Natarajan, *Appl. Organomet. Chem.* 2006, 20, 203.
31. R. Karvembu, K. Natarajan, *Polyhedron* 2002, 21, 219.

33. R. C. Maurya, P. Patel, S. Rajput, Synth. React. Inorg. Met. Org. Chem. 2003, 23, 817.
34. K. N. Kumar, R. Ramesh, Spectrochim. Acta Part A 2004, 60, 2913.
35. M. S. El Shahawi, A. F. Shoair, Spectrochim. Acta part A 2004, 60, 121.
36. R. Ramesh, M. Sivagamasundari, Synth. React. Inorg. Met. Org. Chem. 2003, 33, 899.
37. A. B. P. Lever, Inorganic Electronic Spectroscopy, second ed., Elsevier, New York 1984.
38. K. Chichak, U. Jacquenard, N. R. Branda, Eur. J. Inorg. Chem. 2002, 357.
39. N. Dharmaraj, P. Vishwanathamurthi, P. K. Suganthy, K. Natarajan, Trans. Met. Chem. 1998, 22, 129.
40. M. Muthukumar, S. Sivakumar, P. Viswanathamurthi, R. Karvembu, R. Prabhakaran, K. Natarajan, J. Coord. Chem. 2010, 63, 296.
41. R. Ramesh, S. Maheswaran, J. Inorg. Biochem. 2003, 96, 457.
42. R. Prabhakaran, A. Geetha, M. Thilagavathi, R. Karvembu, V. Krishna, H. Bertagnolli, K. Natarajan, J. Inorg. Biochem. 2004, 98, 2131.
43. Y. Anjuneyula, R. P. Rao, Synth. React. Inorg. Met. Org. Chem. 1986, 26, 257.
44. L. Mishra, V. K. Singh, Ind. J. Chem. 1993, 32A, 446.
45. R. Malhotra, S. Kumar, K. S. Dhindsa, Ind. J. Chem. 1993, 32A, 457.
46. N. Dharmaraj, P. Vishwanathamurthi, K. Natarajan, Trans. Met. Chem. 2001, 26, 105.
47. T. D. Thangadurai, K. Natarajan, Trans. Met. Chem. 2001, 26, 500.
48. T. D. Thangadurai, D. Anitha, K. Natarajan, Synth. React. Inorg. Met. Org. Nano. Met. Chem. 2002, 32, 1329.
49. V. C. Silveira, J. S. Luz, C. C. Oliveira, I. Graziani, M. R. Ciriolo, A. M. C. Ferreira, J. Inorg. Biochem. 2008, 102, 1090.
50. P. Yang, M. L. Guo, B. S. Yand, Chin. Sci. Bull. 1994, 39, 997.
51. E. C. Long, J. K. Barton, Acc. Chem. Res. 1990, 23, 271.
52. L. F. Tan, X. H. Liu, H. Chao, L. N. Ji, J. Inorg. Biochem. 2007, 101, 56.
53. X. Lu, K. Zhu, M. Zhang, H. Liu, J. Kang, J. Biochem. Biophys. Methods 2002, 52, 189.